Available online at www.sciencedirect.com
ScienceDirect
Remote Sensing of Environment 112 (2008) 1603–1613
Remote Sensing of Environment
www.elsevier.com/locate/rse

Classification of sediments on exposed tidal flats in the German Bight using multi-frequency radar data

Martin Gade [a,*], Werner Alpers [a], Christian Melsheimer [b], Gerd Tanck [a]

[a] Universität Hamburg, Zentrum für Meeres-und Klimaforschung, Institut für Meereskunde, Hamburg, Germany
[b] Universität Bremen, Institut für Umweltphysik, Bremen, Germany

Received 1 November 2006; received in revised form 17 August 2007; accepted 18 August 2007

Abstract

We present a new method for the extraction of roughness parameters of sand ripples on exposed tidal flats from multi-frequency synthetic aperture radar (SAR) data. The method is based on the Integral Equation Model (IEM) which predicts the normalized radar cross-section (NRCS) of randomly rough dielectric surfaces. The data used for this analysis were acquired in the German Bight of the North Sea by the Spaceborne Imaging Radar-C/X-Band SAR (SIR-C/X-SAR) in 1994. In-situ measurements of the root-mean-squared (rms) height and the correlation length of the sand ripples clearly demonstrate a relationship between these roughness parameters and the C-band NRCS determined from an ERS SAR image. Using the IEM we have calculated NRCS isolines for the three frequency bands deployed by SIR-C/X-SAR (L, C, and X band), as a function of the rms height and the correlation length of the sand ripples. For each SIR-C/X-SAR image pixel these two roughness parameters were determined from the intersections of the NRCS isolines at different radar bands, and they were used for a crude sediment classification for a small test area at the German North Sea coast. Comparing our results with available sediment maps, we conclude that the presented method is very promising for tidal flat classification by using data from presently existing airborne and future spaceborne multi-frequency SAR systems.

Keywords: Sediment classification; Tidal flats; Radar remote sensing; Integral equation model; Synthetic aperture radar

1. Introduction

Tidal flats are coastal areas that fall dry once during each tidal cycle. Up to a distance of about 10 km offshore, tidal flats dominate the German North Sea Coast (Fig. 1). They are usually non-vegetated and mainly consist of fine sediments such as sand and mud, whereas gravel and shells are rare. The local distribution of these sediments is determined by the velocity of the tidal currents and by the wave action (Allen, 1968). These hydrodynamic forces act on the sediment particles and generate small-scale ripples, whose size and distribution can therefore be related to the distribution of the sediment particles.

The distribution of sediments of a given particle size is of great interest to scientists who work in the field of morpho-dynamics and morphology of coastal environments. However, because of the repetitive flooding and the shallow water depth in these areas, tidal flats are difficult to access both from the sea (by boat) and from land (on foot or by land vehicles), which makes the measurement of soil surface parameters a difficult and time-consuming task. Since remote sensing techniques offer the possibility to examine large areas with very little effort and thus at lower costs, it is a challenging task to conceive a remote sensing technique by which geophysical parameters of tidal flats can be obtained. In particular, radar sensors such as synthetic aperture radar (SAR) operating at different radar bands (frequencies) and flown on airborne or spaceborne platforms can be used for an areal surveillance that is independent of day time and cloud coverage.

The radar backscattering from a soil surface depends on various parameters such as the soil's dielectric constant, its surface roughness, and, if present, its vegetation cover. The combined contribution of these parameters to the radar backscattering, however, makes it difficult to retrieve a single parameter like soil moisture or surface roughness from remotely sensed radar data. Early investigations on the use of radar data for the estimation of soil moisture and roughness were performed by Dobson and Ulaby

* Corresponding author.
E-mail address: martin.gade@zmaw.de (M. Gade).

0034-4257/$ - see front matter © 2007 Elsevier Inc. All rights reserved.
doi:10.1016/j.rse.2007.08.015

(1986) who used data from the Shuttle Imaging radar (SIR)-B mission. In order to derive soil moisture characteristics of bare and vegetated fields O'Neill et al. (1995) used the microwave backscatter models of Shi et al. (1995) and Dubois and van Zyl (1994), together with measured radar copolarization ratios. C band polarimetric observations of soil moisture were performed by Sokol et al. (2002). More recently, Leconte et al. (2004) used Radarsat imagery to produce soil moisture maps of a river basin, and Thoma et al. (2006) compared different approaches to derive estimates of near-surface soil moisture from radar imagery, partly using the Integral Equation Model (IEM) by Fung et al. (1992).

In the particular case of non-vegetated tidal flats the soil moisture is usually very high, so that its contribution to variations of the NRCS can be neglected. This makes it possible to infer the surface roughness parameters, namely, root mean square (rms) height and correlation length, directly from a pair of dual frequency SAR images if a proper backscatter model is used. The IEM developed by Fung et al. (1992) has proven to have a much wider range of applicability to different roughness conditions than classical backscattering models. Therefore, it is widely used as a model for the radar backscattering from soils. Recently, Fung and Chen (2004) included a reflection coefficient in the IEM to improve its applicability in cases of large radar frequencies and roughness scales.

In this paper we use the IEM to develop a method for the extraction of surface roughness parameters of tidal flats from a pair of co-polarized dual frequency SIR-C/X-SAR images. This method, which was first presented in the frame of a Diploma thesis (Tanck, 1998), and later in a Technical Report (Alpers, 1999), is based on an inversion procedure of the IEM.

First results of the use of multi-frequency SAR imagery for the classification of sediments in intertidal ("wadden") areas were presented by Tanck et al. (1999) and by Melsheimer et al. (1999). Van der Wal et al. (2004, 2005) used single-frequency SAR images acquired from aboard the Second European Remote Sensing Satellite (ERS-2) to derive surface roughness and mud content information. In their comprehensive analysis they also applied the IEM and concluded that multi-polarization SAR data or SAR images acquired at different incidence angles would yield more reliable results.

SIR-C/X-SAR has clearly demonstrated that multi-frequency SAR imagery may yield a wealth of information, particularly for terrestrial studies (e.g., Bergen et al., 1997; Pierce et al., 1998), that may not be gained using single-frequency SAR data. So far, SAR sensors aboard satellites (such as ERS, Envisat and Radarsat) operate at a single frequency, thus making it impossible to use multi-frequency SAR imagery on a routine basis. However, in addition to the C band SARs flying presently on ERS; Envisat, and Radarsat satellites, presently also an L band SAR (PALSAR) is flying on the Japanese ALOS satellite and in the near future X band SARs will fly on the German TerraSAR-X and the Italian COSMOS-Skymed satellites. By combining SAR

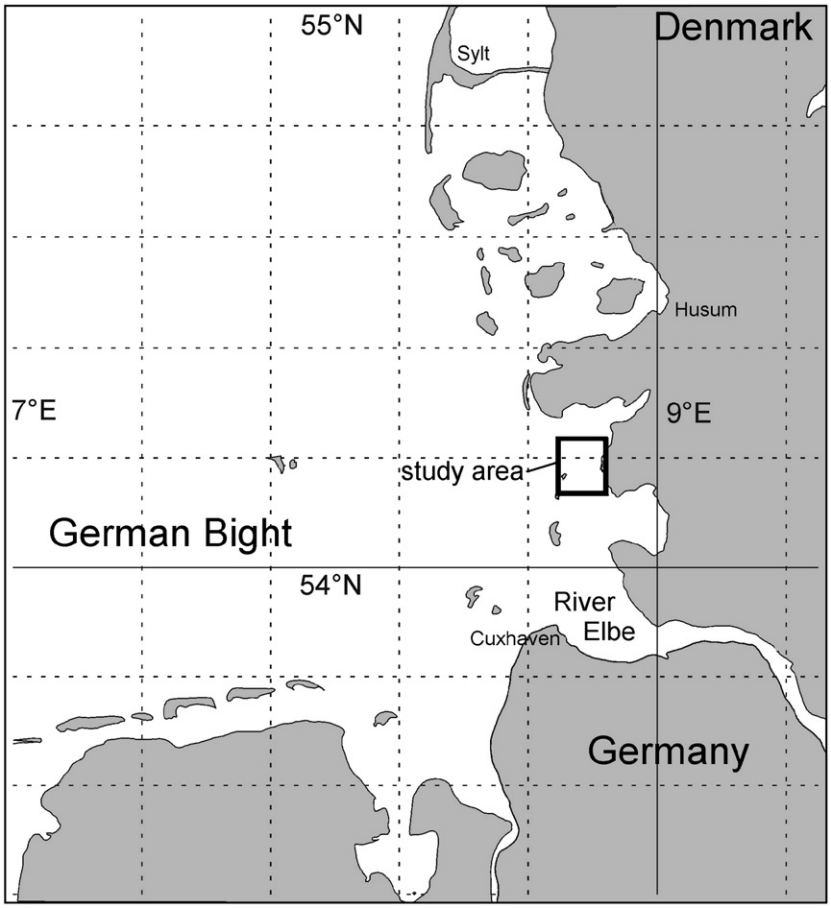

Fig. 1. Map of the German North Sea coast (160 km × 180 km). The study area is marked by the black rectangle.

images acquired by these satellites at different radar frequencies, information on tidal flats may be obtained by using the method proposed in this paper. But simultaneous acquisition of multi-frequency SAR data from different satellites is hardly possible. However, multi-frequency SAR images acquired at the same phase of the tidal cycle could be combined.

But the best way of obtaining information on tidal flats by using our proposed method is the use of simultaneously acquired multi-frequency airborne SAR data. At present there exist several airborne SAR systems capable of collecting such data, e.g., the German E-SAR and the Russian IMARC.

In the next chapter we present SIR-C/X-SAR images acquired in 1994 that were used for the IEM inversion, and we summarize the results from in-situ measurements carried out in 1998, simultaneously to an ERS SAR image acquisition. The IEM and the theoretical background for our analyses are described in the subsequent chapter, followed by a presentation of the main results of our inversion procedure.

2. SAR data and in-situ measurements

In order to derive surface roughness parameters with sufficient accuracy through an inversion of the IEM, SAR data acquired simultaneously at different radar frequencies are needed. So far, only SIR-C/X-SAR has provided such a data set from spaceborne SAR sensors. Our investigation comprises in-situ measurements that were carried out in 1998, i.e., about four years after the shuttle missions. Since the sediment distribution in the study area was likely to have changed during that time, we used an ERS SAR image acquired at the time of our field campaign in 1998 for a direct comparison of the in-situ data and SAR data.

2.1. Study area

The study area "Wesselburener Watt" in the German Bight (North Sea) is shown in Fig. 2. It is located between the mouth of the river Eider (in the north) and the city of Büsum (in the south), between 54.12°N and 54.26°N, and 8.66°E and 8.86°E. The area is covered mainly by sandy and mixed (sandy/muddy) sediments, whose distribution strongly depends on the local hydrodynamic forces. In general, large-particle sediments are found close to the low-tide waterline and to the tidal creeks, whereas small-particle sediments are found on the open flats. Mudflats are rare and are found only along the coastline.

2.2. SAR data

During two SIR-C/X-SAR missions in April and October, 1994, three SARs operating at different radar frequencies, 1.25 GHz (L band), 5.3 GHz (C band), and 9.6 GHz (X Band), were flown on board the space shuttle "Endeavour". Whereas X-SAR (X band) operated only at VV polarization (vertically transmitted, vertically received), SIR-C (L and C band) operated in a fully polarimetric mode providing images at the four polarization combinations HH, VV, VH, and HV. For more detailed information see Table 1. The data used for the analysis presented herein were acquired on April 10, 1994, at 0805 UTC,

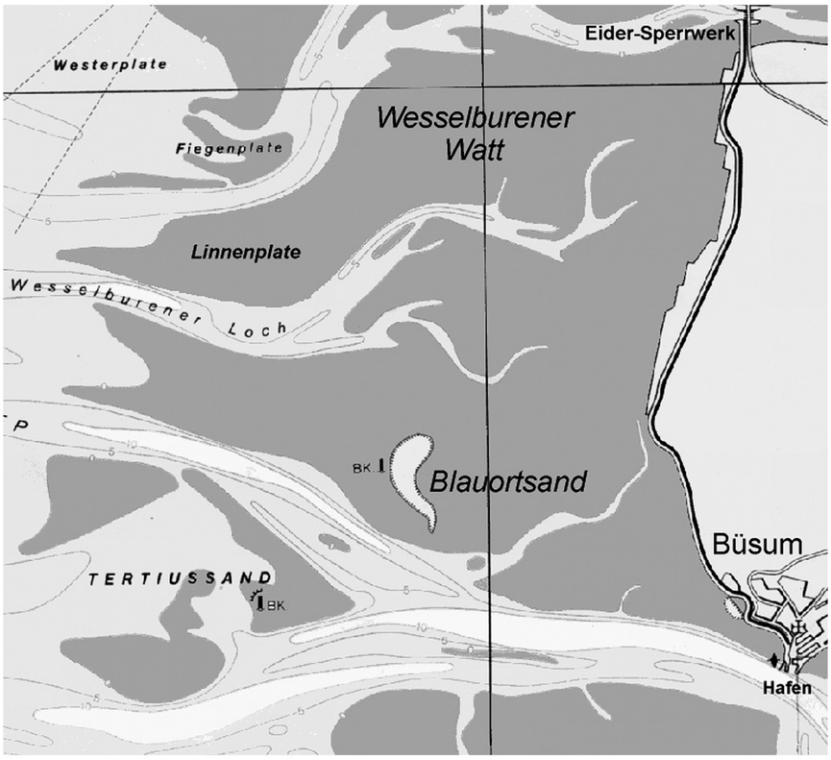

Fig. 2. Map (15 km × 13.5 km) of the study area "Wesselburener Watt", located north-west of the city of Büsum. The major tidal creeks are marked in light grey. In the lower image center the sandbank "Blauortsand" is located.

Table 1
SIR-C/X-SAR and ERS SAR sensor characteristics

Platform	Sensor	Pixel size	Frequency (Radar band)	Polarization
Spaceshuttle Endeavor	SIR-C	12.5 m	1.25 GHz (L)	HH, VV,
			5.30 GHz (C)	VH, HV
	X-SAR	12.5 m	9.60 GHz (X)	VV
ERS-2	SAR	12.5 m	5.30 GHz (C)	VV

which was 2 h and 45 min after low tide in the study area. Weather stations in Husum and Cuxhaven (located north and south of the study area, respectively, see Fig. 1) reported a mean wind speed of 5.7 m/s and a mean (easterly) wind direction of 100°, at the time of SAR data acquisition. Fig. 3 shows three SIR-C/X-SAR images of the same area shown in Fig. 2 (black rectangle in Fig. 1), that were acquired at L band (upper left), C band (upper right), and X band (lower right) at VV polarization. The pixel size of the SAR images is 12.5 m. Note that at L band (left image) exposed tidal flats appear much darker on the image than open water and land areas, whereas at C and X band tidal flats appear sometimes both darker and brighter than open water and land areas.

The in-situ studies described herein were performed in 1998, i.e., about 4 years after the space shuttle missions. Because of the high morpho-dynamics in that area (i.e., the strong dynamical change in morphology and/or soil sediments) it was unlikely that the sediment distribution had not changed since the shuttle flights in 1994. Therefore, we used for comparison an image acquired by the SAR aboard the European Remote Sensing Satellite (ERS-2, see Table 1). In Fig. 4a) a 15.0 km × 13.5 km subset of the ERS-2 SAR image is shown that was acquired on April 4, 1998, at 1045 UTC (23 min before low tide), simultaneously with the field campaign. At the time of the in-situ measurements, the mean wind speed was 6.0 m/s and the mean wind direction was 225°. The ERS-2 SAR is operating at C band, and the texture in Fig. 4 is very similar to the texture of the same area imaged by the C-band SAR depicted in the upper right panel of Fig. 3 (the pixel sizes are the same). A smaller section (3.0 km × 2.4 km) of this image is

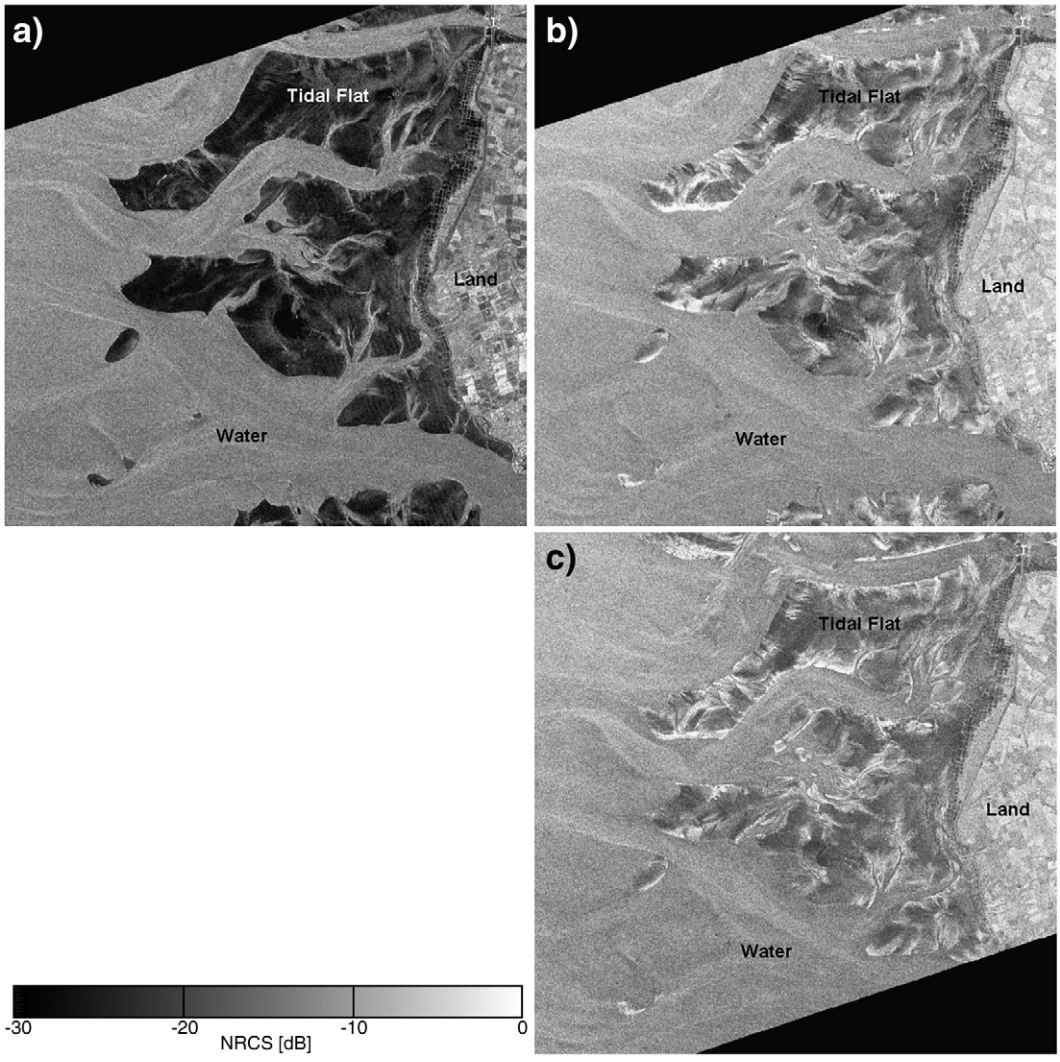

Fig. 3. SIR-C/X-SAR images of the study area acquired at (a) L band, VV polarization, (b) C band, VV polarization, and (c) X band, VV polarization. Images acquired from spaceshuttle Endeavor during the SIR-C/X-SAR mission on April 10, 1994, at 0805 UTC, 2 h 45 min after low tide. Image dimensions: 12 km × 12 km.

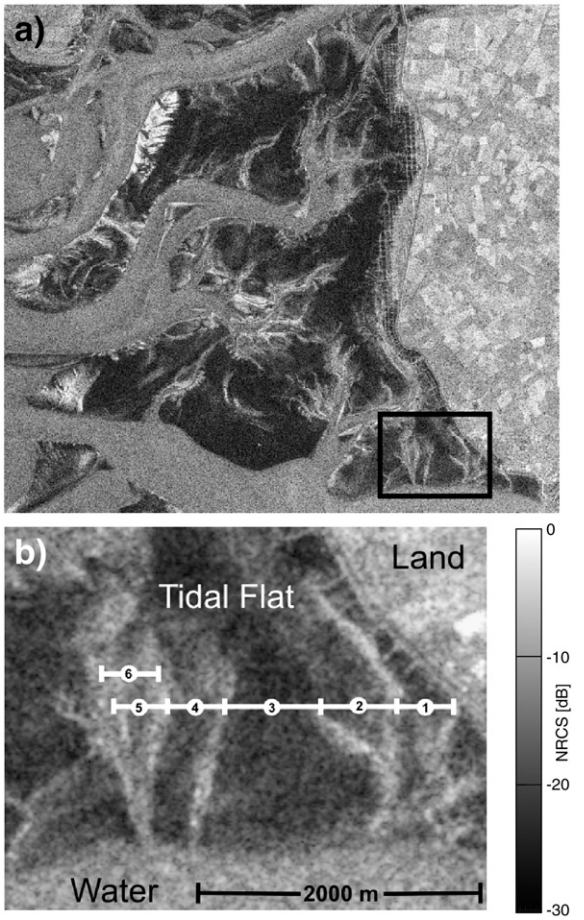

Fig. 4. a) subset (15.0 km × 13.5 km) of the C-band ERS-2 SAR image of the study area, acquired on April 4, 1998, at 1045 UTC (23 min before low tide). b) 3.0 km × 2.4 km section of the above image (see the black rectangle). At the time of the ERS-2 SAR image acquisition, in-situ measurements were performed along the tracks marked white in the lower image (and sub-divided into 6 sections).

shown in Fig. 4b), with the track inserted (marked white) along which the in-situ measurements of the surface roughness were performed (see below).

2.3. In-situ measurements

In order to get a set of reference data of the soil surface parameters concurrent with an ERS-2 SAR image acquisition, in-situ measurements were conducted on April 4, 1998, in the study area. Soil samples taken at 18 different locations revealed soil moisture between 38% and 50% per unit volume (volumetric moisture). The average volumetric soil moisture was measured to be 43%. For the measurement of surface roughness profiles we used a self-constructed sledge equipped with a profiling sensor that was following the ground contour while the sledge was hand-towed along an east-western track. The sensor generated a frequency-modulated (FM) signal, whose frequency was proportional to the local surface height and which was continually recorded on magnetic tape. The positioning was carried out by using a handheld Global Positioning System (GPS) receiver. With this sensor several surface profiles of a total length of about 2500 m were measured. Fig. 4 shows a subset of the ERS-2 SAR image acquired at the time of the in-situ measurements, with the measurement tracks inserted.

We subdivided the tracks along which the roughness measurements were performed into six individual sections each starting and ending at a water-filled tidal creek that could not be passed by the sledge. It is well known (see, e.g., Ehlers, 1988) that the stream velocity of the tidal currents is higher near the tidal creeks than on the open flats. As a result, the surface roughness, and therefore the NRCS in the vicinity of the creeks, is also increased. This effect is clearly visible in the ERS-2 SAR image depicted in Fig. 4 where the neighborhood of the tidal creeks is imaged significantly brighter than the surrounding area. Note that at the time of SAR image acquisition, the width of the tidal creeks in the study area was 5 m or less, thus they were not resolved in the SAR image, whose pixel size is 12.5 m. Fig. 5 shows the NRCS values derived from the ERS-2 SAR image (upper panel) and the rms height and correlation length obtained from the sledge measurements along the same line (middle and lower panel, respectively).

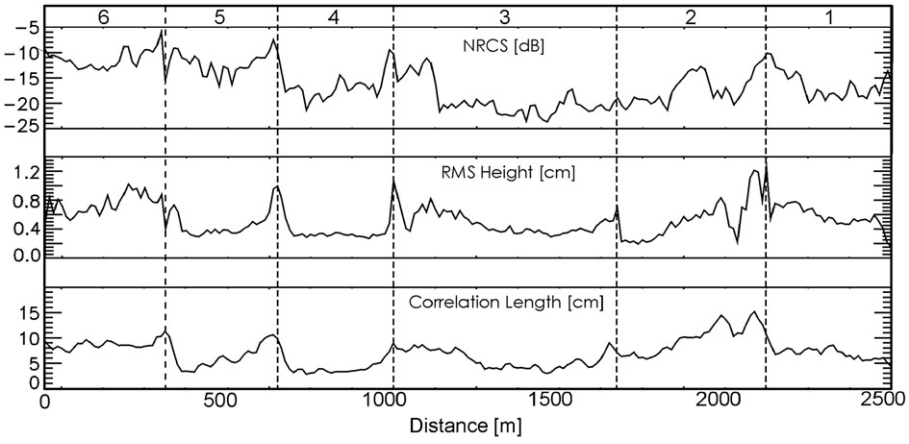

Fig. 5. Upper panel: NRCS values derived from the ERS-2 SAR image along the track inserted in Fig. 4; middle and lower panel: rms height and correlation length, respectively, measured from the hand-towed sledge simultaneously to the ERS-2 SAR image acquisition. The numbering on the top corresponds to the subsections marked in Fig. 4. The boundaries between the subsections (dashed vertical lines) are the positions of tidal creeks.

Local variations in (large-scale) surface slope may also be responsible for an increase in NRCS (Fung et al., 1992), if the surface is tilted towards the radar, thus resulting in a steeper local incidence angle for the microwaves. However, in the C and X band SAR images shown in Fig. 3 bright regions (of increased NRCS) are found at various locations that are likely to be tilted in different directions (i.e., towards the tidal creeks nearby). Thus, we assume that the local slope is not a dominant factor determining the radar backscattering from tidal flats.

The mean value of the NRCS of the tidal flats in between the creeks is about −20 dB, while in their vicinity it is up to −5 dB (see Fig. 4). This behavior is clearly correlated with the measured rms height (middle panel of Fig. 5): the rms height in between the creeks and in their vicinity is about 0.4 cm and 1.2 cm, respectively.

During the experiment we found that a certain amount of water stays in the sand ripple troughs such that they were half-filled with water. This water effectively reduces the surface roughness seen by the incident microwaves (because they are backscattered from the water surface), but this was not measured by the sensor mounted on the sledge. We shall discuss this effect in more detail later when we compare the measured roughness data with those inferred from the model inversion.

2.4. Inversion method

Since the mean (rms) slope of ripples on tidal flats is small, single scattering dominates over multiple scattering in most cases. Moreover, surface scattering dominates the volume scattering, because (1) the soil moisture of tidal flats is high and the high conductivity of sea water causes the penetration depth of the electromagnetic waves at L, C, and X band to be smaller than 10% of the wavelength, and (2) the soil can be considered homogeneous, without dielectrical discontinuities (where volume scattering can occur). A suitable model for this kind of surface scattering is the Integral Equation Model (IEM) introduced by Fung et al. (1992).

The IEM predicts the NRCS of bare soil as a function of its dielectric constant and surface roughness. The latter is generally described by the autocorrelation function and the standard deviation of the roughness height (rms height). According to

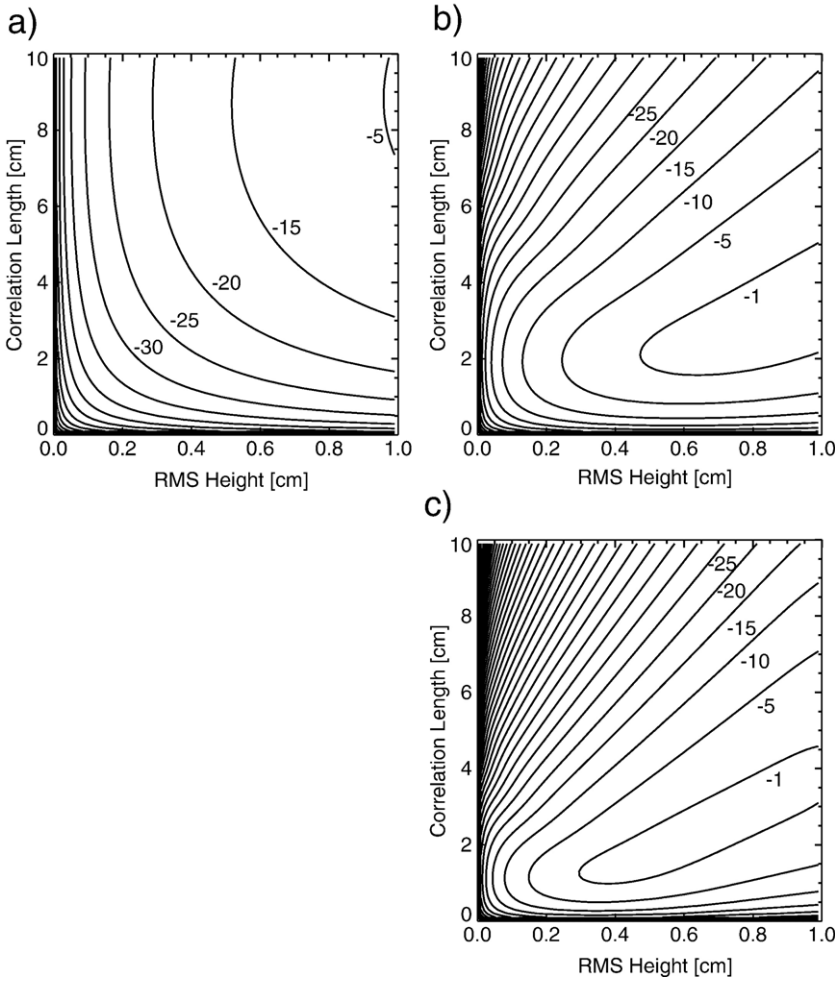

Fig. 6. Isolines of the NRCS values (in dB) derived applying the IEM for (a) L band, VV polarization, (b) C band, VV polarization, and (c) X band, VV polarization, for a sand ripple profile with Gaussian autocorrelation function.

Fung et al. (1992) the single-scattering term of the IEM for vertical (VV) polarization, σ^0_{vv}, can be expressed as:

$$\sigma^0_{vv} = \frac{k^2}{2}\exp(-2k_z^2h^2)\sum_{n=1}^{\infty} h^{2n}|I^n_{vv}|^2\frac{W^n(-2k_x,0)}{n!} \quad (1)$$

where

$$I^n_{vv} = (2k_z)^n\frac{2R_{||}}{\cos\vartheta}\exp(-h^2k_z^2) + \frac{k_z^n[F_{vv}(-k_x,0)+F_{vv}(k_x,0)]}{2},$$

k is the radar wavenumber (with components k_x and k_z in the ground range and vertical direction, respectively), h is the rms surface height, W^n is the Fourier transform of the n-th power of the surface autocorrelation function, and ϑ is the radar incidence angle. $R_{||}$ is the Fresnel reflection coefficient for parallel polarization (i.e., in the plane of incidence), and F_{vv} is a field coefficient for vertically polarized scattering described in detail by Fung et al. (1992).

Our surface profiles measured by the sledge-mounted sensor indicate that the surface autocorrelation function of tidal flats is very similar to a Gaussian autocorrelation function. This is plausible because ripples found on tidal flats always have smoothly shaped rounded forms. Therefore, we may assume for the theoretical calculations of the backscattering coefficients of tidal flats a Gaussian autocorrelation function of the surface. The sensitivity of the NRCS predicted by the IEM to changes of the soil moisture is generally very low for volumetric water contents larger than 30% and saturates at higher values (Shi et al., 1997; Wang & Schmugge, 1980). Simulations of the NRCS at L, C, and X band by applying the IEM show that large variations of the dielectric constant cause only minor changes in the NRCS. The difference between the NRCS for soil with a volumetric moisture of 40% and the NRCS for sea water having the same surface roughness as the soil is only of the order of 1 dB. In contrast, a reduction of the rms height by 50% leads to a reduction of the NRCS of about 10 dB. Since we measured in our study area an average soil moisture of the sand of 43%, it is predominantly the surface roughness rather than the soil moisture that determines the strength of the backscattered radar signal. In other words: the NRCS of tidal flats depends mainly on the rms height and correlation length. Thus, the theoretical values of the NRCS at different radar bands can be presented as two-dimensional charts. Fig. 6 shows the calculated isolines of the NRCS of tidal flats at the three SIR-C/X-SAR radar bands: (a) L band, (b) C band, and (c) X band. The soil dielectric constant is estimated using values measured by Hallikainen et al. (1985).

The principle of the inversion is as follows: each pixel in a SAR image has an NRCS value that, for a given radar frequency, lies on a certain isoline derived with the IEM. If SAR images of the same resolution cell (acquired at the same time) are available at two suitable radar frequencies, estimates of the roughness parameters, rms height and surface correlation length, can be determined from the intersection of the two associated isolines of the theoretical NRCS.

As an example Fig. 7 shows the three isolines (calculated with the IEM) that correspond to NRCS values derived from collocated pixels in the three SIR-C/X-SAR images of a selected position on the tidal flats (−18 dB at L band, −9 dB at C band, and −11 dB at X band). Note that the isolines for C band and X band (Panels b and c, respectively, of Fig. 6) are quite similar compared to those for L band (Panel a of Fig. 6). This is in accordance with Fig. 3, where the C and X band SAR images show very similar textures of the tidal flats. Therefore, we suggest that L band images, in combination with either C band or X band images, are best suited for deriving soil-surface roughness parameters when applying the IEM inversion method. In the case of SIR-C/X-SAR data, however, L band and C band images are the optimum combination, because these SAR images are already collocated in the SIR-C/X-SAR data set.

3. Results and discussion

By applying the inversion procedure based on the IEM we have obtained maps of the rms height and correlation length of the study area in the German Bight. The speckle in the SAR data was reduced by applying a Lee filter. Open water was masked using a supervised maximum likelihood classifier, and a land mask was applied manually. The results are depicted in Fig. 8, where the upper row contains the results for the entire study area, and the lower row contains results for the sub-area where the in-situ measurements were performed in 1998 (see Fig. 4). Note that rms heights above 0.4 cm (left panels of Fig. 8) are particularly encountered near the tidal creeks and the open water where the current velocity and wave action is increased, while low rms heights are encountered on the level and smooth flats, away from the creeks. Correlation lengths above 4 cm (right panels of Fig. 8) are mainly found in areas of reduced hydrodynamic forces, i.e., near the coastline and in the center of the tidal flats, away from the creeks.

At the locations where the in-situ surface roughness data were collected in 1998 the inversion yields an average rms

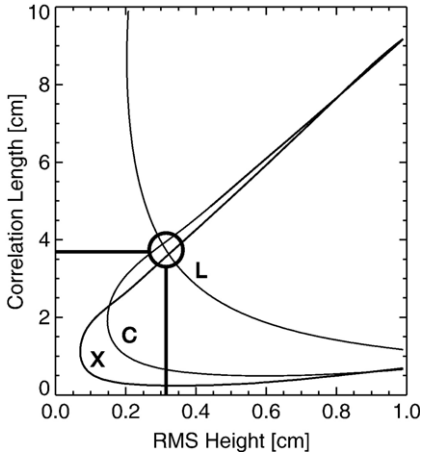

Fig. 7. Example of the inversion process. At a given position on the tidal flats the NRCS values at L-, C-, and X-band are −18 dB, −9 dB, and −11 dB, respectively. The three isolines of the NRCS were calculated applying the IEM as a function of rms height and correlation length. Their intersection point denotes the rms height and correlation length derived for that position (image pixel).

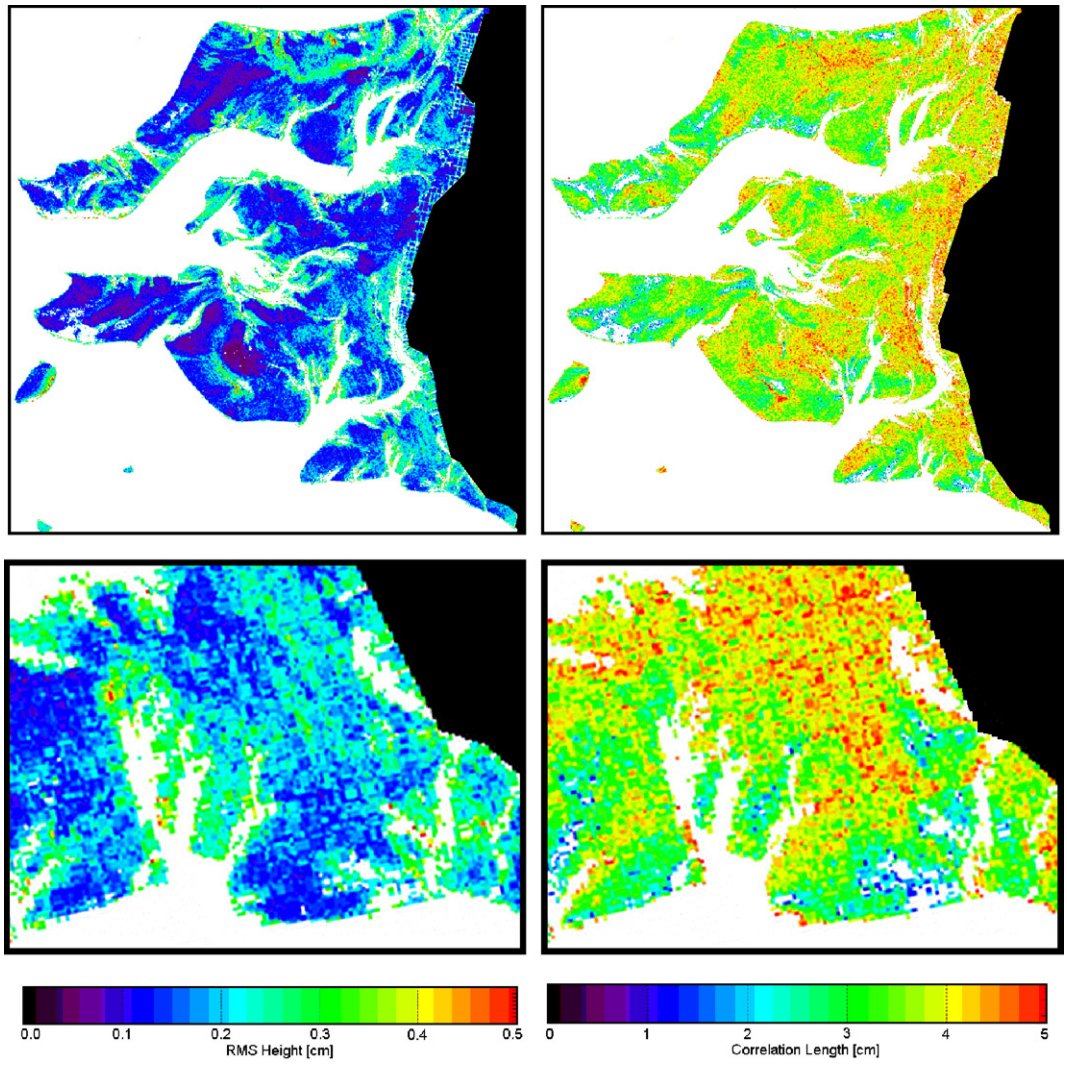

Fig. 8. Left column: rms height maps of the tidal flats as a result of the inversion of SIR-C/X-SAR data using the IEM. Right column: correlation length maps obtained by the same inversion process. The lower two panels show the same subset as Fig. 4b). In all panels open water has been masked white.

height of approximately 0.2 cm, see the lower left panel of Fig. 8. This is in good agreement with the value obtained from the in-situ measurements, if we assume that the rms height of tidal flats is reduced by the water residing in the ripple troughs. In order to demonstrate the effect of remnant water on the calculated rms height, we have used a measured surface profile and simulated an increased water level, see Fig. 9. The profile length is 2.5 m with (relative) surface heights varying between −2.5 cm and −5 cm, and the simulated water level is −3.5 cm, so that the water covers about 30% of the tidal flat's surface. Without water the calculated rms height is 0.35 cm, and with the remnant water it is only 0.21 cm. This example clearly shows the strong effect of the remaining water on the derived surface roughness parameters. Assuming that the situation was similar at the time of the in-situ measurements, the rms height inferred from the SIR-C/X-SAR images may have to be doubled, leading to a value of approximately 0.4 cm, which is close to the in-situ measured value of 0.43 cm.

The retrieval of correlation lengths from the inversion procedure results in values between 0.9 cm and 7.3 cm, with

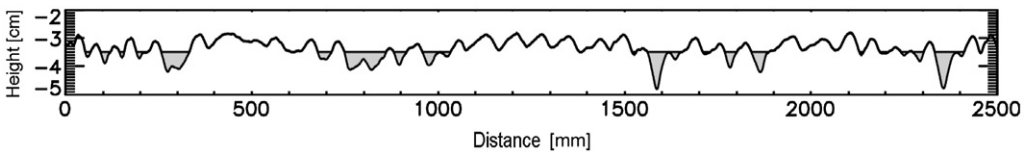

Fig. 9. Measured surface profile of an exposed tidal flat with a simulated mean water level of −3.5 cm (the zero-point of the measurements was chosen arbitrarily). Note that the water covers only 30% of the surface, but it reduces the calculated rms height by 40%.

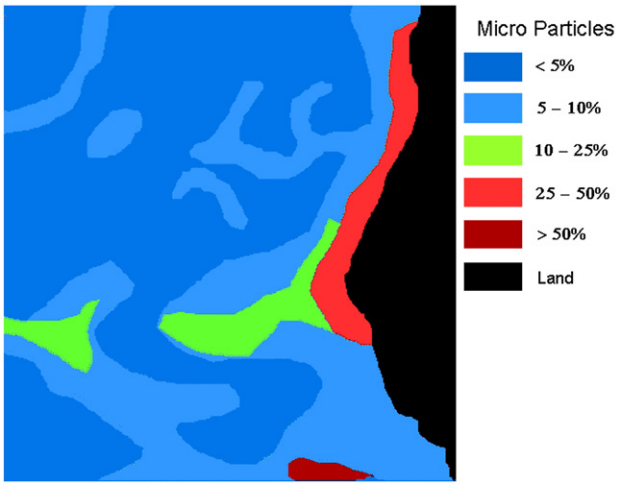

Fig. 10. Sediment classification provided by the Schleswig Holstein Wadden Sea National Park Office. The color coding denotes the percentage of micro particles (i.e., particles with diameters less than 63 μm).

most of the values lying between 3.0 cm and 5.0 cm. The in-situ measurements of the correlation length (see Fig. 5) yields values between 0.2 cm and 23 cm with an average value of 6.9 cm. Note that the long time period of 4 years between the SIR-C/X-SAR image acquisition and the collection of the in-situ data suggests that the values are not directly comparable. Nevertheless, a quantitative comparison reveals that the inversion process seems to underestimate the overall surface correlation length generally by a factor of 0.6. For the further analyses and for the sediment classification (see below) we have corrected our results for this factor.

In summary, the estimated rms heights derived from the SAR data agree reasonably well with the rms heights derived from the in-situ measurements, while the correlation lengths obtained from the SAR data seem to be too low compared to the values obtained from the in-situ measurements. The reason for this difference is probably the particular form of the surface autocorrelation function that was used in the calculation of the NRCS: for a given NRCS value a Gaussian correlation function results in a much shorter correlation length than an exponential correlation function.

The surface roughness parameters derived from the SAR data were used for a crude sediment classification in the study area. The sediment map shown in Fig. 10 was provided by the Schleswig Holstein Wadden Sea National Park Office and was obtained from samples taken during several in-situ campaigns.

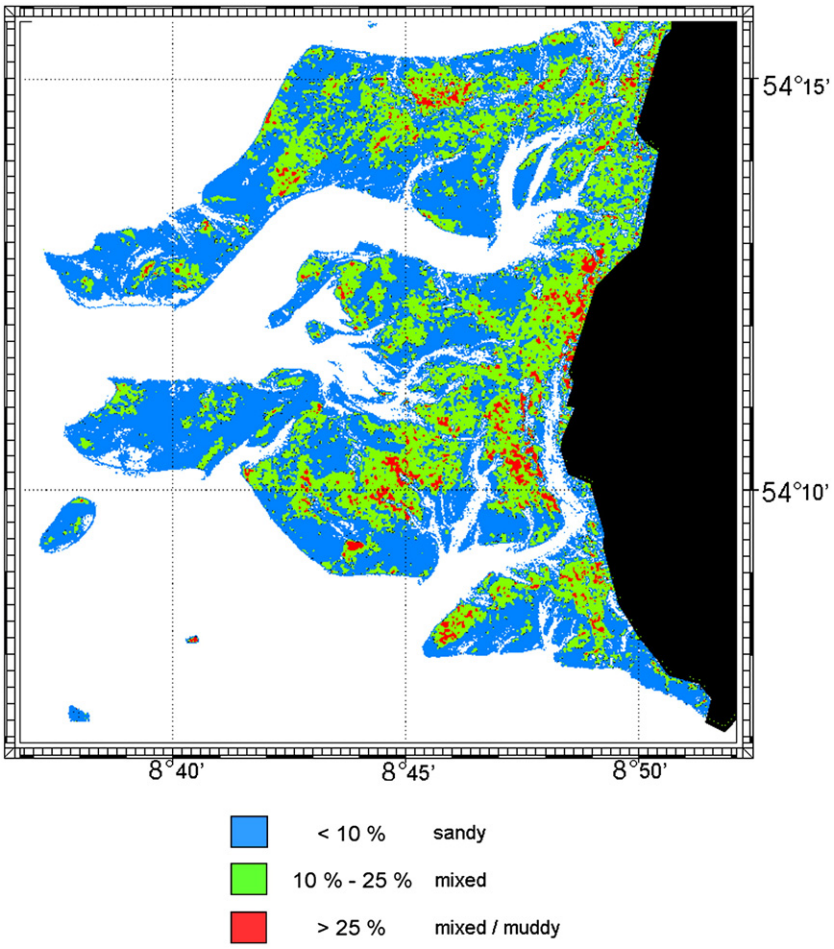

Fig. 11. Sediment classification inferred from the SIR-C/X-SAR data (Fig. 3) through the inversion process based on the IEM. The three classes denote different percentages of micro particles (diameters less than 63 μm).

The sediments are classified in terms of percentage of micro particles, i.e., the volumetric fraction of small particles with diameters less than 63 μm. Depending on the sediment type, dry-fallen tidal flats are usually covered with ripples by only 10–70% (Kleeberg, 1990). This implies that, in general, the rms height is usually not well suited for the classification of sediment types. Therefore, we have used a relationship between the correlation length and the sediment type proposed by Pröber (1981): in general, sediments are grouped as sandy, mixed, and mixed/muddy, according to the content of micro particles of less than 10%, between 10% and 25%, and greater than 25%, respectively. The transition correlation length between sandy and mixed soil and between mixed and mixed/muddy soil is 3.7 cm and 4.2 cm, respectively.

Fig. 11 shows the crude sediment classification based on the results of the inversion process, namely on the above relationship between sediment types and the derived correlation lengths. In general, the open tidal flats are dominated by mixed/muddy soil (micro-particle content less than 25%), whereas the vicinities of the tidal creeks are dominated by sandy soil (micro-particle content less than 10%). At a first glance, this looks like an artifact of the applied method. However, the sediment map provided by the National Park Office shows some coarse qualitative agreement with the results presented herein. Particularly the areas of high percentages of micro particles agree very well (red and green areas in Figs. 11 and 10).

4. Summary and conclusions

We have presented a new method based on the inversion of the single-scattering Integral Equation Model (IEM) model to provide estimates of the two surface roughness parameters used to characterize tidal flats: the rms height and the correlation length of the sand ripple profiles. The roughness parameters have been derived from a pair of dual-frequency, co-polarized synthetic aperture radar (SAR) images that were acquired simultaneously during the Spaceborne Imaging Radar-C/X Band (SIR-C/X)-SAR missions in 1994 over tidal flats at low tide in the German Bight of the North Sea. These results have been compared with those obtained from in-situ measurements performed in 1998 in the same area.

Our method is based on two main assumptions: firstly, the NRCS of dry-fallen tidal flats is mainly governed by the profile of the sand ripples, and secondly, the parameters characterizing this profile, rms height and correlation length, can be considered as proxies for the sediment type. Our results show evidence that these assumptions are valid for our study area. However, further studies performed in different intertidal zones will be needed to gain further insight and to demonstrate whether or not the proposed method is limited to our region of interest.

The rms heights derived from the SAR data and those measured in-situ agree reasonably well. However, the correlation lengths derived from the SAR data are lower than the measured ones, which is probably due to the particular form of the surface autocorrelation function used in our calculations. Therefore, we hypothesize that the optimum form of the autocorrelation function of the surface roughness of tidal flats is a hybrid function (which is very close to the Gaussian form, though). Note that this study can only be seen as a rough sketch of the proposed method for later operational use.

Another problem for the retrieval of surface roughness data from SAR images is the water that remains in the ripple troughs on the flats. Ryu et al. (2002) have presented photographs of exposed tidal flats with remaining water in sand ripples and mud patches (see their Fig. 1). The amount of this remnant water depends not only on the topography of the tidal flats, but also on exposure time and local weather conditions (Ryu et al., 2002, 2004). At the first instance, the thin water layer causes the surface roughness experienced by an incident microwave to be underestimated. Moreover, the water layer's surface roughness depends on wind speed and may affect the total NRCS of the tidal flat. However, since the size of the water patches in the ripple troughs is usually small (a few centimeters in diameter), we assume that in our case the influence of wind-induced surface waves on the radar backscattering is negligible, particularly at L and C band.

The comparison of the retrieved results with an existing sediment map has shown that the proposed method is working fairly well, if the surface of the exposed tidal flats is dominated by sand ripples. However, the available data cannot be used to investigate whether or not the suggested inversion method can be applied for tidal flats with predominant muddy sediments. Moreover, since the thickness of the water layer is quite variable in space and time, it may be difficult to draw any detailed conclusions on the soil surface roughness on the basis of the proposed inversion method. More detailed studies on its applicability should be performed in future, when data from satellite-borne SAR sensors operating at L, C, and X band (PALSAR on ALOS, ASAR on ENVISAT, and TerraSAR-X, respectively) will be available. Future investigations should be devoted to (1) the analysis of radar data acquired at different polarizations (horizontal and cross-polarization), (2) the use of additional microwave frequencies, and (3) in-situ measurements performed simultaneously with the acquisition of the multi-frequency microwave data.

We note that data from different satellites cannot easily be combined if they are acquired with a considerable time lag in between. A much deeper knowledge of the radar backscatter properties of the sediment types, and its dependence on weather conditions, tidal cycle, and imaging geometry will be needed, which can only be gained from dedicated experimental campaigns, e.g., with airborne sensors and simultaneous in-situ measurements.

Acknowledgments

The authors would like to thank A. Kellermann of the Schleswig Holstein Wadden Sea National Park Office in Tönning for providing the sediment classification map. This work was funded by the German Federal Ministry of Education and Research under contracts 50 QS 9016 ("X-SAR/SIR-C") and 03 EE 9714 ("XEP").

References

Allen, J. R. L. (1968). *Current ripples; their relation to patterns of water and sediment motion.* Amsterdam: North Holland Publishing Company. 433 pp.

Alpers, W. (1999). *XEP, Klassifizierung von Wattgebieten unter Verwendung von X-SAR/SIR-C-Daten. Abschlussbericht.* Bonn: Deutsches Zentrum für Luft-und Raumfahrt (DLR). 23 pp.

Bergen, K. M., Dobson, M. C., & Pierce, L. E. (1997). Effects of within-season dielectric variations on terrain classification using SIR-C/X-SAR. *Proceed. Intern. Geosci. Remote Sens. Sympos. (IGARSS) '97* (pp. 1072−1074).

Dobson, M., & Ulaby, F. (1986). Preliminary evaluation of the SIR-B response to soil moisture, surface roughness, and crop canopy cover. *IEEE Transactions on Geoscience and Remote Sensing*, *24*(4), 517−526.

Dubois, P., & van Zyl, J. (1994). An empirical soil moisture estimation algorithm using imaging radar. *Proceed. Intern. Geosci. Remote Sens. Sympos. (IGARSS) '94* (pp. 1573−1575).

Ehlers, J. (1988). *The morphodynamics of the Wadden Sea.* Rotterdam: Balkema. 397 pp.

Fung, A. K., & Chen, K. S. (2004). An update on the IEM surface backscattering model. *IEEE Geoscience and Remote Sensing Letters*, *1*, 75−77.

Fung, A. K., Li, Z., & Chen, K. S. (1992). Backscattering from a Randomly Rough Dielectic Surface. *IEEE Transactions on Geoscience and Remote Sensing*, *30*, 356−369.

Hallikainen, M. T., Ulaby, F. T., Dobson, M. C., El-Rayes, M. A., & Wu, L. -K. (1985). Microwave dielectric behaviour of wet soil — Part I: Empirical models and experimental observations. *IEEE Transactions on Geoscience and Remote Sensing*, *23*, 25−34.

Kleeberg, U. (1990). *Kartierung der Sedimentverteilung im Wattenmeer durch integrierte Auswertung von Satellitendaten und Daten aus der Wattenmeer-datenbank der GKSS, Diplomarbeit, Fachbereich Geographie/Geowis-senschaften, Universität Trier, Trier, Germany.* 115 pp.

Leconte, R., Brissette, F., Galarneau, M., & Rousselle, J. (2004). Mapping near-surface soil moisture with RADARSAT-1 synthetic aperture radar data. *Water Resources Research*, *40*, W01515. doi:10.1029/2003WR002312

Melsheimer, C., Tanck, G., Gade, M., & Alpers, W. (1999). Imaging of tidal flats by the SIR-C/X-SAR multi-frequency/multi-polarisation synthetic aperture radar. In G. J. A. Nieuwenhuis, R. A. Vaughan, & M. Molenaar (Eds.), *Operational remote sensing for sustainable development* (pp. 189−192). Rotterdam: Balkema.

O'Neill, P. E., Hsu, A. Y., & Shi, J. C. (1995). Soil moisture estimation using time-series radar measurements of bare and vegetated fields in Washita '92. *Proceed. Int. Geosci. Remote Sens. Sympos. (IGARSS) '95* (pp. 498−500).

Pierce, L. E., Bergen, K. M., Dobson, M. C., & Ulaby, F. T. (1998). Multi-temporal land-cover classification using SIR-C/X-SAR imagery. *Remote Sensing of Environment*, *64*, 20−33.

Pröber, C. (1981). Die Möglichkeit der Fernerkundung in der Küstengeologie, Dissertation, Fachbereich Mathematik-Naturwissenschaften, Universität Kiel, Kiel, Germany.

Ryu, J. H., Na, Y. H., Won, J. S., & Doerffer, R. (2004). A critical grain size for Landsat ETM+ investigations into intertidal sediments: a case study of the Gomso tidal flats, Korea. *Estuarine, Coastal and Shelf Science*, *60*, 491−502.

Ryu, J. H., Won, J. S., & Min, K. D. (2002). Waterline extraction from Landsat TM data in a tidal flat: A case study in Gomso Bay, Korea. *Remote Sensing of Environment*, *83*, 442−456.

Shi, J., Wang, J., Hsu, A. Y., O'Neill, P. E., & Engman, E. T. (1997). Estimation of bare surface soil moisture and surface roughness parameter using L-band SAR image data. *IEEE Transactions on Geoscience and Remote Sensing*, *35*, 1254−1266.

Shi, J., Wang, J., O'Neill, P., Hsu, A., & Engman, E. (1995, Jan. 17–20). Application of IEM Model to soil moisture and surface roughness estimation. *Proceed. NASA/JPL AIRSAR Workshop, JPL, Pasadena, CA*.

Sokol, J., Pultz, T. J., Deschamps, A., & Jobin, D. (2002). Polarimetric C-band observations of soil moisture for pasture fields. *Proceed. Intern. Geosci. Remote Sens. Sympos. (IGARSS) '02* (pp. 1532−1534).

Tanck, G. (1998). *Untersuchungen der Radarrückstreueigenschaften unterschiedlicher Wattypen des schleswig-holsteinischen Wattenmeeres mit Hilfe eines Multi-frequenz/Multipolarisations-SAR, Diplomarbeit, Fachber-eich Physik, Universität Hamburg, Hamburg, Germany.* 101 pp.

Tanck, G., Alpers, W., & Gade, M. (1999). Determination of surface roughness parameters of tidal flats from SIR-C/X-SAR 3-frequency SAR data. *Proceed. Intern. Geosci. Remote Sens. Sympos. (IGARSS) '99* (pp. 194−196).

Thoma, D. P., Moran, M. S., Bryant, R., Rahman, M., Holifield-Collins, C. D., Skirvin, S., et al. (2006). Comparison of four models to determine surface soil moisture from C-band radar imagery in a sparsely vegetated semiarid landscape. *Water Resources Research*, *42*, W01418. doi:10.1029/2004WR003905

Van der Wal, D., Herman, P. M. J., & Ysebaert, T. (2004). Space-borne synthetic aperture radar of intertidal flat surfaces as a basis for predicting benthic macrofauna. *EARSeL eProceedings*, *31*, 69−80.

Van der Wal, D., Herman, P. M. J., & Wielemaker-van den Dool, A. (2005). Characterisation of surface roughness and sediment texture of intertidal flats using ERS SAR imagery. *Remote Sensing of Environment*, *98*, 96−109.

Wang, J. R., & Schmugge, T. J (1980). An empirical model fort he complex dielectric permittivity of soil as a function of water content. *IEEE Transactions on Geoscience and Remote Sensing*, *18*, 288−295.